

Development of a Mesh Refinement Process for the Prediction of Propeller Tip Vortex Cavitation

Ronan Doherty, James Alderton and William Batten
QinetiQ, Haslar Maritime Technology Park, Gosport, United Kingdom
rldoherty@qinetiq.com

1 Introduction

Cavitation occurs when the fluid pressure drops below the local vapour pressure and is often an inevitable phenomenon for hydro machinery. It can have a detrimental impact on power and performance and is therefore a major limiting factor in the design of marine propulsors. The low pressure core of a strong propeller tip vortex can initiate tip vortex cavitation, which can lead to excessive noise and vibration, as well as causing erosion to the propulsor and surrounding structures. Of particular importance is the noise signature associated with the inception of a tip vortex cavity, which can pose a significant threat to ocean wildlife, particularly to marine mammals which rely on sound for communication. Development of accurate and reliable techniques for the numerical prediction of tip vortex cavitation has therefore become an area of growing interest in recent years, as has been the assessment of the application of commercial CFD codes to cavitating propeller flows.

From the relevant literature it can be seen that prediction of the tip vortex cavity depends strongly on the mesh resolution within the vortex region (Szantyr *et al.* 2011, Fujiyama *et al.*, 2011). Mesh refinement approaches have thus far focused on fixed volumetric refinements behind the propeller tip, requiring *a priori* knowledge of the flow field, and a mesh refinement cell size of $D_{\text{Prop}}/1000$ has been employed to resolve part of the tip vortex cavity (Yilmaz, 2017). Given the computationally demanding requirements on the mesh, and the current limitations of the cavitation models, it is noted that there are still difficulties in numerically predicting the full extent of the downstream tip vortex cavity when using commercial CFD codes (Usta *et al.*, 2018). In order to predict the conditions for the onset of cavitation for full scale vessels, a reliable scaling law to scale from model tests to full scale propellers for cavitation inception is required. Deriving a suitable scaling law for cavitation inception using CFD has also been an area of interest within cavitation research (Hsiao *et al.*, 2008, Shen *et al.*, 2009).

The aim of this study was to develop a mesh refinement process for the numerical prediction of tip vortex cavitation, using the commercial CFD package STAR-CCM+. Given the strong dependence on the mesh resolution within the areas of interest, this study focuses on mesh refinement, and the use of field functions for adaptive meshing are investigated. The process should be able to capture the minimum pressure within the tip vortex core and should be applicable to different types of hydrodynamic propulsors, at both model and full scale. Additionally, to limit pre-processing time, an overly manual process should be avoided and it should therefore be easily automated. It is also hoped that the mesh refinement process can be used to investigate the effect of scaling on tip vortex cavitation inception.

2 Development of the Mesh Refinement Process



Fig. 1: Still from case 2.3.2.

Propeller diameter, D_{Prop}	0.25m
Advance Ratio, J	1.269
Cavitation number, σ_n	1.424
Density, ρ	997.59 kg/m ³
Dynamic viscosity, μ	9.4472E-04 Pa.s
Inlet velocity	7.93 m/s
Outlet pressure	30516.47 Pa
Propeller RPM	1500

Table 1: PPTC case 2.3.2 conditions.

The Potsdam Propeller Test Case (PPTC) is a 5-bladed model scale propeller which has been experimented on in both cavitating and non-cavitating conditions by the SVA Potsdam Model Basin.

The results were released as part of the 2011 Symposium on Marine Propulsors (smp'11) as validation data to aid the development of numerical methods for calculation of the performance of marine propulsors (Barkmann *et al.*, 2011). Case 2.3.2 from the cavitating experiments was chosen as an ideal case for the development of the refinement process, since in this case tip vortex cavitation visibly occurs, as can be seen in Fig. 1. The flow conditions for this case are shown in Table 1.

The flow solver used was STAR-CCM+ 13.04.011, and the simulations were run in steady state conditions with a single water phase. The rotation of the propeller was modelled using a rotating reference frame. The RANS (Reynolds Averaged Navier Stokes) K-Omega SST turbulence model was used with an all y^+ wall treatment. A single blade passage was modelled using periodic boundaries, as the blades were assumed to be identical, and a polyhedral mesh was used for the propeller blade passage. The computational domain and the single blade passage boundaries are shown in Figs. 2 and 3, respectively.

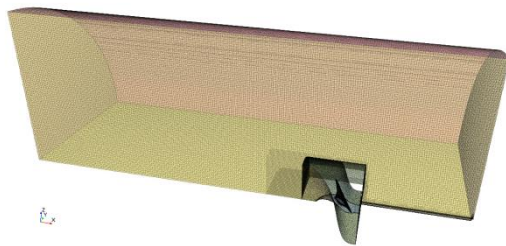


Fig. 2: Full computational domain.

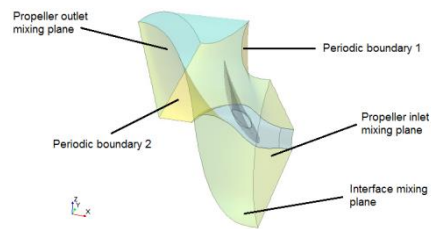


Fig. 3: Single blade passage boundary conditions.

The mesh refinement table method was investigated by firstly obtaining an initial converged solution on a coarse mesh and then defining a mesh refinement x,y,z , position table based on field function criteria. This table is then used to define cell sizes, and the domain is re-meshed before continuing the simulation. However, this method was deemed unsuitable, as the tables do not partition well on multiple cluster cores. The resulting mesh contained large cell volume gradients and poor quality cells, and this led to poor convergence of the solution.

As a result, an alternative method was explored; threshold part volumetric refinement. As before, an initial converged solution is obtained on a coarse mesh and from this solution threshold parts are defined based on field functions of interest. These threshold parts are saved as STL files and imported into the simulation, and the surface is then wrapped using the surface wrapper tool to ensure a closed volume. The wrapped surface can then be used to define volumetric refinements. The simulation continues on the refined mesh until convergence is achieved, and the refinements are repeated iteratively, reducing the refinement cell sizes on each iteration, until convergence of the minimum vortex pressure is achieved. This method has numerous advantages over the mesh refinement table method as thresholds of scalars are easy to construct and export, the volumetric refinements will efficiently mesh in parallel and the resulting mesh is of good quality since volumetric growth rates can be utilised.

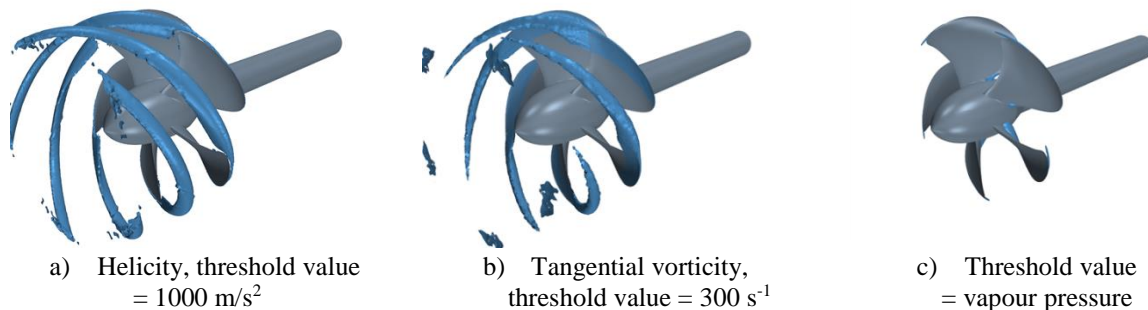


Fig. 4: Thresholds of the assessed field functions.

Once the initial solution had been run on the initial coarse mesh, multiple field functions were assessed to determine which of these could effectively delineate the tip vortex region, and to determine what threshold values should be used. To ensure that the refinements would only be applied to the blade tip, the field functions were filtered so as to only be defined within the region $0.8 < \text{radial}$

co-ordinate/propeller radius < 1.1. The field functions assessed were helicity, tangential vorticity and absolute pressure, which are shown in Fig. 4. From the assessment, it was decided that a two-tier refinement strategy would be employed, with refinements applied to the region with tangential vorticity $> 300\text{s}^{-1}$, and a finer refinement applied to the region below the vapour pressure, $P < 2771\text{Pa}$. The volumetric refinement cell sizes were reduced by 25% on each iteration, and the volumetric refinements for iterations two, four and six are shown in Figs. 5 and 6. It can be seen that as the mesh is refined, the absolute pressure volumetric refinement region grows, indicating that the tip vortex is being resolved further downstream as the mesh is refined. Fig. 7 shows the pressure coefficient and the mesh within the tip vortex, just downstream of the blade. It is observed that as the mesh is refined, the vortex core pressure decreases, since the tip vortex is better resolved.



Fig. 5: Tangential vorticity volumetric threshold refinements for iterations two, four and six. Cell sizes are $D_{\text{Prop}}/320$, $D_{\text{Prop}}/640$ and $D_{\text{Prop}}/960$, respectively.

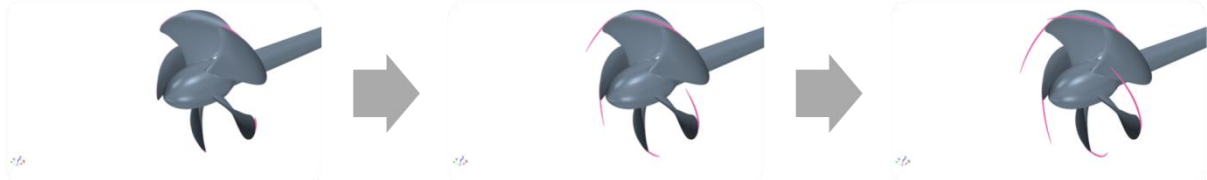


Fig. 6: Absolute pressure volumetric threshold refinements for iterations two, four and six. Cell sizes are $D_{\text{Prop}}/640$, $D_{\text{Prop}}/1280$ and $D_{\text{Prop}}/2880$, respectively.

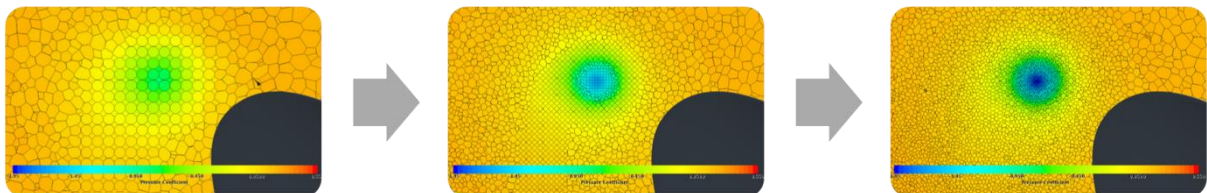


Fig. 7: The refined mesh and pressure coefficient within the tip vortex for iterations two, four and six.

Fig. 8 shows the convergence of the total volume of cells below vapour pressure, throughout the refinement process. Annotations R1 to R6 denote the mesh refinement iterations. Fig. 9 shows the vortex core pressure coefficient at two locations downstream of the propeller, and the minimum pressure coefficient within the vortex, $C_{p_{\text{min}}}$. Vortex monitor locations 1 and 2 lie on the plane which intersects the propeller centre line and lies parallel to the x- and z-axes, with vortex location 2 lying one full propeller tip vortex rotation downstream. From Fig. 8, convergence of the volume below vapour pressure is achieved by the fifth tip vortex mesh refinement, R5. Fig. 9 shows that convergence is achieved for the vortex core pressure coefficients at locations 1 and 2.

From the experimental data, a thrust coefficient, K_T , of 0.2450 was obtained for the non-cavitating open water case, and a value of 0.2064 for the cavitating case. For the most refined mesh, R6, a K_T value of 0.2458 was calculated. Since cavitation was not modelled in the CFD, this value is compared to the non-cavitating experiment, and a difference of 0.33% is obtained. Monitoring K_T throughout the refinements, it was observed that the tip vortex refinements did not have a significant impact.

3 Application of the Mesh Refinement Process to Scaled-Up Propellers

The refinement process was applied to two scaled up PPTC cases, representative of a medium scale and a full scale propeller. The propeller diameter was scaled up by a factor of six and fifteen to yield the medium and full scale propeller diameters, respectively. The simulation conditions were obtained

by ensuring cavitation number and advance ratio similarity, and are shown in Table 2. The fluid properties of the two larger propellers are representative of seawater at 15 degrees.

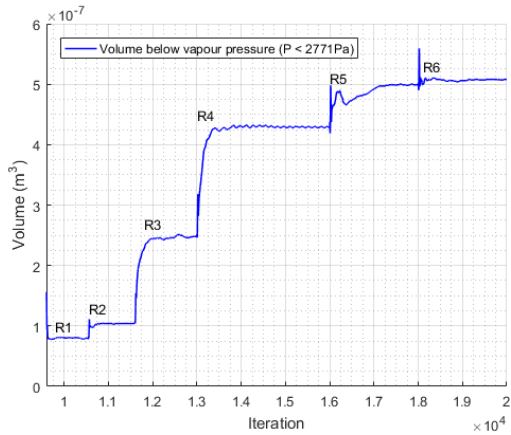


Fig. 8: Monitor of volume below vapour pressure.

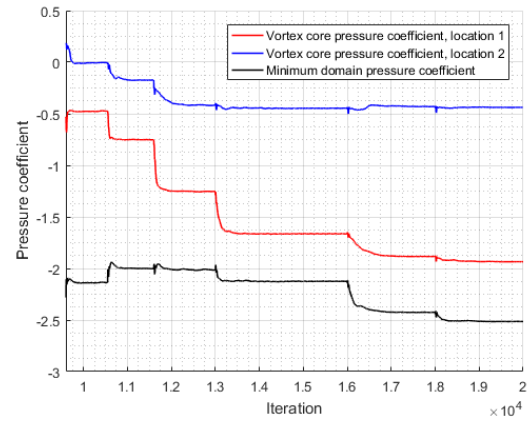


Fig. 9: Monitors of the vortex core pressure coefficients at two locations downstream of the blade, and the minimum domain C_p .

Table 2: Scaled up propeller dimensions and flow conditions.

	Model Scale	Medium Scale	Full Scale
D_{Prop} (m)	0.25	1.5	3.75
ρ (kg/m ³)	997.59	1025.07	1025.07
μ (Pa.s)	9.4472E-04	1.1030E-03	1.1030E-03
U_∞ (m/s)	7.93	9.774	13.376
P_{Out} (Pa)	30516.47	46085.23	83880.19
RPM	1500	308.14	168.67

It was found that the tangential vorticity threshold value could be non-dimensionalised using the propeller diameter and the inlet velocity, whilst maintaining the same relative refinement volume at all scales. A normalised tangential vorticity threshold value of 9.5 was employed in all cases. The absolute pressure threshold remained the same for all cases, as the fluid vapour pressure was assumed to be unchanged. Figs. 10 and 11 show the monitored values throughout the refinement process for the Full scale propeller.

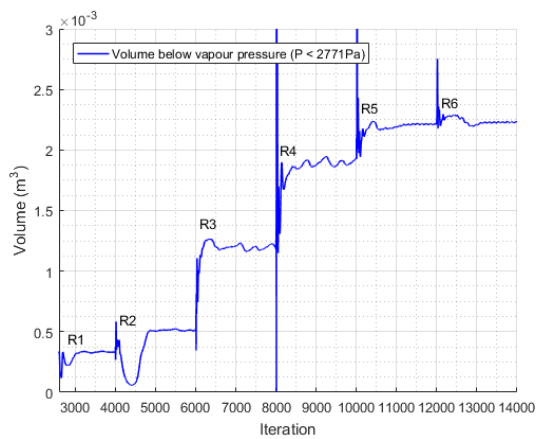


Fig. 10: Monitor of volume below vapour pressure for the full scale propeller.

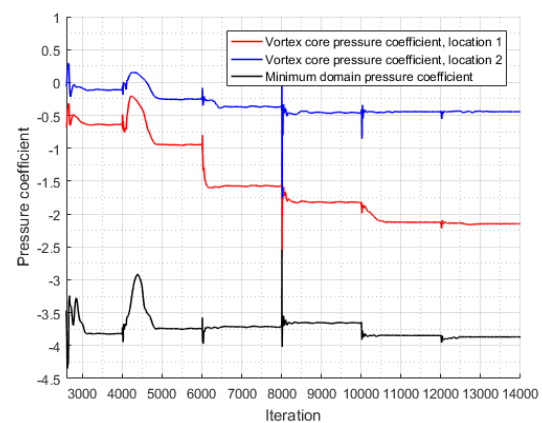


Fig. 11: Monitors of the vortex core pressure coefficients at two locations downstream of the blade, and the minimum domain C_p .

The convergence behaviour remains more or less unchanged when compared to the model scale convergence (Figs. 8 and 9) however it can be seen that the converged pressure coefficient values are lower for the full scale propeller. To further investigate these differences, the pressure coefficient was

plotted through the tip vortex at location 1 for both the model and full scale propellers, and these are shown in Figs. 12 and 13. The distance from the vortex centre has been normalised by propeller diameter in each case.

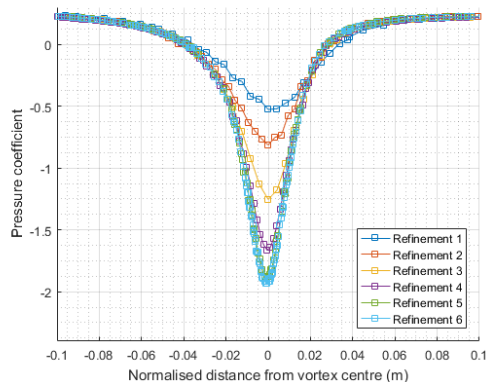


Fig. 12: Plot of C_p across the model scale vortex core.

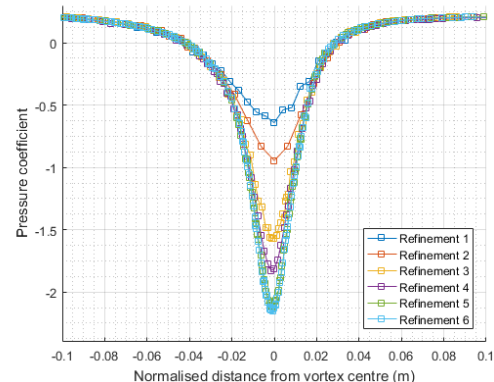


Fig. 13: Plot of C_p across the full scale vortex core.

These Figures show that the vortex core pressures have converged by R6 as there is very little change between the R5 & R6 mesh plots. It is observed that the free stream pressure coefficient is the same in both cases, which is expected as both were run at the same cavitation number, and the relative size of the vortex core remains the same. As observed in Fig. 11, the minimum pressure coefficient is lower for the full scale propeller.

4 Cavitation inception scaling

As the refinement process has been applied to different propeller scales, a cavitation inception scaling law can be investigated. Assuming the cavitation inception number is $-C_{p_{min}}$, a scaling law can be defined according to Eq. 1.

$$\frac{\sigma_{i,2}}{\sigma_{i,1}} = \frac{-C_{p_{min,2}}}{-C_{p_{min,1}}} = \left(\frac{Re_2}{Re_1}\right)^\gamma \quad (1)$$

There have been numerous studies investigating the appropriate scaling parameter, γ , that should be used, and these can be compared to that found using the refinement process. The classical constant for γ was calculated by McCormick for a hydrofoil tip vortex, and was found to be 0.4 (McCormick, 1962). However, recent studies have shown that this value is applicable only to the laminar flow regime, and that γ should increase with Reynolds number, Re . Eq. 2 shows a relation for γ based on turbulent boundary layer theory, which is dependent on Re (Shen *et al.*, 2009).

$$\gamma = \frac{5.16 \log\left(\frac{\log Re_2}{\log Re_1}\right)}{\log\left(\frac{Re_2}{Re_1}\right)} \quad (2)$$

Table 3 shows Re and the tip vortex $C_{p_{min}}$ obtained from the refinement process for the three propeller scales and Table 4 shows the γ value obtained from the refinement process and from Eq. 2.

Table 3: Re and tip vortex $C_{p_{min}}$ for the three propeller scales.

	Model Scale	Medium Scale	Full Scale
Re	1.745×10^6	18.91×10^6	38.87×10^6
Tip $C_{p_{min}}$	-2.514	-3.510	-3.869

It can be seen that the values obtained from the refinement process are much lower than the classical value of 0.4, as the flow within the propeller tip vortex at this Re range is highly turbulent. The γ values obtained from the refinement process are also lower than those predicted by Eq. 2. However, the trend is the same, indicating that the refinement process results capture the Re dependency of the scaling law. Hsiao *et al.* (2008) performed a CFD study on small, medium and large scaled propellers,

representing Re numbers of 2.09×10^6 , 4.19×10^6 and 8.38×10^6 , using both RANS and DNS (Direct Numerical Simulation) approaches. Values for γ of 0.33 and 0.15 were obtained for the scaling of small to medium and medium to large scales, respectively, using RANS. The DNS simulations yielded lower $C_{p_{min}}$ values, and γ values of 0.22 and 0.11 were obtained. These results also display a general trend for γ to decrease as Re increases. As the refinement process simulations were performed at larger Re , the values obtained by the refinement process are not unreasonable when compared to the higher Re scaling values obtained by Hsiao *et al.* of 0.15 (RANS) and 0.11 (DNS). It must be noted that only single phase simulations have been run in this study, and there is evidence that γ is adjusted back closer to the classical value of 0.4 when nuclei effects are modelled, provided that a statistical cavitation inception criterion is used and is not too stringent (Hsiao et al. 2008.)

Table 4: Comparison between the CFD obtained scaling law and Shen's scaling law (Eq. 2.)

Re_1	Re_2	Re Ratio	CFD γ	Shen's γ
18.91×10^6	38.87×10^6	2.055	0.135	0.302
1.745×10^6	18.91×10^6	10.836	0.140	0.332
1.745×10^6	38.87×10^6	22.267	0.139	0.325

7 Conclusions

A mesh refinement process for the prediction of tip vortex cavitation has been developed and applied to both the model scale PPTC and scaled up propellers. The process achieved convergence of the minimum vortex core pressures, $C_{p_{min}}$, for RANS simulations at the three propeller scales to which it was applied. A cell size of $D_{prop}/2880$ was required within the tip vortex core for a converged $C_{p_{min}}$ for all scales. It was also found that the tangential vorticity field function threshold could be non-dimensionalised to achieve the same relative refinement volume at all scales. The converged $C_{p_{min}}$ values obtained by the refinement process reduced as the scale and Re increased, which allowed for a prediction of the cavitation inception scaling parameter, γ . The scaling parameter obtained from the refinement process grew smaller with increasing Re , which is in agreement with recent analytical and numerical studies. In the future, the refinement process should be applied to higher fidelity simulation methods such as DES (Detached Eddy Simulation), and the effect of modelling multiphase cavitation on the refinement process and on the predicted cavitation inception scaling parameter should also be investigated.

Acknowledgements

The authors acknowledge the UK MoD for supporting the research and development through the Maritime Strategic Capability Agreement.

References

- U. Barkmann, H-J. Heinke and L. Lubke. "Potsdam Propeller Test Case (PPTC) Description", Second International Symposium on Marine Propellers smp'11, Hamburg, Germany, June 2011.
- K. Fujiyama, C.H. Kim and D. Hitomi. "Performance and Cavitation Evaluation of Marine Propeller using Numerical Simulations". Second International Symposium on Marine Propulsors (smp'11), Hamburg, Germany, 2011.
- C.-T. Hsiao and G. L. Chahine. "Scaling of Tip Vortex Cavitation Inception for a Marine Open Propeller". 27th Symposium on Naval Hydrodynamics, Seoul, Korea, 5-10 October 2008.
- B.W. McCormick, "On Cavitation Produced by a Vortex Trailing from a Lifting Surface". *ASME Journal of Basic Engineering*, vol 84, pp. 369-379, 1962.
- Y.T. Shen, S. Jessup, S. Gowing, "Tip Vortex Cavitation Inception Scaling for High Reynolds Number Applications". *Journal of Fluids Engineering*, vol. 131(7), 2009.
- J. Szantyr, P. Flaszynski, K. Tesch, W. Suchecki and A. Alabrudzinski. "An Experimental and Numerical Study of Tip Vortex Cavitation". *Polish Maritime Research*, vol.18, pp. 14-22, 2011.
- O. Usta and E. Korkut, "A study for cavitating flow analysis using DES model". *Ocean Engineering*, vol. 160, pp. 397-411, 2018.
- N. Yilmaz , M. Khorasanchi and M. Altar, "An Investigation into Computational Modelling of Cavitation in a Propeller's Slipstream", Fifth International Symposium on Marine Propulsion (smp'17), Espoo, Finland, 2017.